

Quantum Langevin molecular dynamics determination of the solar-interior equation of state

Jiayu Dai, Yong Hou, and Jianmin Yuan*

Department of Physics, College of Science, National University of Defense Technology,
Changsha 410073, P. R. China

Received _____; accepted _____

*Corresponding author, E-mail:jmyuan@nudt.edu.cn

ABSTRACT

The equation of state (EOS) of the solar interior is accurately and smoothly determined from *ab initio* simulations named quantum Langevin molecular dynamics (QLMD) in the pressure range of $58 \leq P \leq 4.6 \times 10^5$ Mbar at the temperature range of $1 \leq T \leq 1500$ eV. The central pressure is calculated, and compared with other models. The effect of heavy elements such as carbon and oxygen on the EOS is also discussed.

Subject headings: equation of state — solar interior — *ab initio*

1. Introduction

For solar and stellar models, a high-quality equation of state (EOS) is very crucial (Basu & Antia 2008). It is well-known that some requirements should be satisfied for solar and stellar modeling: thermodynamic quantities would be smooth, consistent, valid over a large range of temperature and density, and incorporate the most important astrophysically relevant chemical elements (Däppen 2006) as well. There are two major efforts for a high-precision and high-accuracy EOS made before, which have been included in the recent opacity recalculations. They are the international Opacity Project (OP) (Seaton 1995; Berrington 1997) and Opacity Project at Livermore (OPAL). In OP, the model named Mihalas-Hummer-Däppen (MHD) (Hummer & Mihalas 1988; Mihalas et al. 1988; Däppen et al. 1988; Nayfonov et al. 1999; Trampedach et al. 2006) for EOS is developed, dealing with *heuristic* concepts about the modification of atoms and ions in a plasma. In the other one, OPAL, the EOS relies on *physical picture*, which is built on the modeling of electrons and nuclei. This model is called ACTEX (activity expansion) EOS (Rogers 1986; Rogers et al. 1996; Rogers & Nayfonov 2002; Iglesias & Rogers 1991). Both MHD and OPAL are dependent on the potentials between particles (electron-electron, ion-electron, ion-ion). In addition, there are other models such as Eggleton, Faulkner, & Flannery (1973) (EFF), which is thermodynamically consistent and qualitatively correct. EFF does not consider excited states, H molecule formation, or Coulomb corrections, and treats full ionization for heavy elements at high density. It is interesting to note that the effect of partially degenerate electrons can be included partly according to the Fermi-Dirac statistics. In most cases, the EOS from OP, OPAL and even EFF should be good for the input parameters of stellar models. However, there is always some physics such as the coupling of ions which is missed in these models. With the increasing requirements of the high-precision in helioseismic study, a parameter-free model beyond Debye-Hückel approximation for a more accurate EOS than that of OPAL and MHD is still necessary (Däppen 2006; Däppen &

Nayfonov 2000).

The conditions in the solar interior are very complicated, where the densities are from 10 g/cm³ up to 160 g/cm³, and temperatures from 50 eV to 1400 eV (Bahcall et al. 2001). At the same time, Hydrogen and Helium are the main elements, taking about 98%, with small abundances of other heavy elements such as carbon, oxygen and iron. In order to obtain an accurate and smooth EOS for the whole sun, it is necessary to develop a model which can cover all conditions in the sun. It is very clear that matter in the sun is not always ideal ionized gas plasma, but moderately coupled, partly degenerate, and partly ionized (especially for heavy elements) in some area according to the definition of coupling parameter Γ and degenerate parameter θ (Ichimaru 1982), where $\Gamma = Z^{*2}/(k_B T a)$, with T the system temperature, k_B the Boltzmann constant, a the mean ionic sphere radius defined as $a = (3/(4\pi n_i))^{1/3}$, Z^* the average ionization degree, n_i the ionic number density, and $\theta = T/T_F$, with the Fermi temperature $T_F = (3\pi^2 n_e)^{2/3}/2$ (n_e is the number density of electrons). Generally speaking, when the degenerate parameter $\theta \sim 1$ and coupled parameter $\Gamma \sim 1$, the matter is considered to be partially degenerate and moderately coupled. Otherwise, if $\theta \ll 1$ ($\theta \gg 1$) and $\Gamma \gg 1$ ($\Gamma \ll 1$), matter is strongly (weakly) degenerate and strongly (weakly) coupled. For most of regimes in solar interior, matter is weakly coupled and weakly degenerate. However, the extremely high density can not promise the negligibility of the coupling of ions, and the theory of ideal ionized gas plasma is not always appropriate. For weakly coupled or weakly degenerate matter, single atomic models such as average atoms (AA) models (Hou et al. 2006; Yuan 2002), and detailed level accounting (DLA) (Zeng & Yuan 2004) are assumed valid. Generally, AA model is built for the dense plasma, and DLA model is available for the relatively low density. Very recently, AA model was applied for the astrophysical plasmas successfully (Faussurier et al. 2010). However, there is no direct physical evidence supporting these approaches, and we don't even know whether they are correct in such dense matter, and how they behave for the

extreme dense matter under conditions such as the solar center. Therefore, it is extremely important to develop a more reliable model for all these conditions.

For the strongly (moderately) coupled matter with partly degenerate electrons, quantum molecular dynamics (QMD), without requiring any assumptions about the potential between atoms, supplies a powerful and accurate tool, and has been successfully applied in warm dense matter (WDM) (Collins et al. 1995; Desjarlais et al. 2002; Mazevet et al. 2005, 2008). In astrophysics, QMD has been used to study the properties of giant planets and given rise to amazingly satisfying results (Lorenzen et al. 2009; Militzer & Hubbard 2009; Gillan et al. 2006; Vorberger et al. 2007; Nettelmann et al. 2008; Wilson & Militzer 2010). Very recently, QMD was extended to the field of high energy density physics (HEDP) by considering the electron-ion collision induced friction (EI-CIF) in the procedure of molecular dynamics, and the corresponding model called quantum Langevin molecular dynamics (QLMD) was constructed (Dai & Yuan 2009; Dai et al. 2010). Thanks to this model, one can go into the regime of HEDP from first principles, and the thermodynamic properties of the sun and sun-like stars can be therefore researched based on *ab initio* method. It also gives us a good tool to investigate the system in which the coupling of ions is important.

In this work, we firstly study the EOS of conditions under the solar interior using QLMD. Three densities with different temperatures are chosen, and their EOS are compared with the EOS of the AA model with energy-level broadening (AAB) (Hou et al. 2006). QLMD can ensure much more accurate results in all conditions, and agrees with AAB at high temperatures. The central pressure of the sun is also calculated using different models, comparing with the data of other models and standard solar models (Bahcall et al. 2001). The important effect of heavy elements on EOS of very dense matter is also investigated at the end.

2. Theoretical method

2.1. Quantum Langevin molecular dynamics

We firstly recall the QLMD method here, where the electronic structure is studied from density functional theory (DFT), and the ionic trajectory is performed using Langevin Equation ([Dai et al. 2010](#))

$$M_I \ddot{\mathbf{R}}_I = \mathbf{F} - \gamma M_I \dot{\mathbf{R}}_I + \mathbf{N}_I, \quad (1)$$

Where M_I is the ionic mass, \mathbf{F} is the force calculated in DFT, γ is a Langevin friction coefficient, \mathbf{R}_I is the position of ions, and \mathbf{N}_I is a Gaussian random noise corresponding to γ . Considering the dynamical collisions between electrons and ions at high temperature, the friction coefficient γ can be estimated by

$$\gamma = 2\pi \frac{m_e}{M_I} Z^* \left(\frac{4\pi n_i}{3} \right)^{1/3} \sqrt{\frac{k_B T}{m_e}} \quad (2)$$

Where m_e is the electronic mass, Z^* , n_i and T are the same as the above definition. Therefore, the dynamical electron-ion collisions at high temperature can be described as a friction or noise effect. By introducing this dynamical EI-CIF, the first principles simulations can be applied in the HEDP regime, overcoming the difficulty of numerical calculations, and therefore give more reliable results.

To guarantee an accurate sampling of the Maxwell-Boltzmann distribution, the noise has to obey the fluctuation-dissipation theorem:

$$\langle \mathbf{N}_I(0) \mathbf{N}_I(t) \rangle = 6\gamma M_I k_B T dt \quad (3)$$

Where dt is the time step of molecular dynamics. At the same time, the random forces are taken from a Gaussian distribution of mean zero and variance of $\langle \mathbf{N}_I^2 \rangle = 6\gamma M_I k_B T / dt$.

In order to integrate Eq. 1, the formalism in a Verlet-like form ([Pastor et al. 1988](#))

integration is performed as follows

$$\begin{aligned} \mathbf{R}_I(t + dt) = & \mathbf{R}_I(t) + (\mathbf{R}_I(t) - \mathbf{R}_I(t - dt)) \frac{1 - \frac{1}{2}\gamma_T dt}{1 + \frac{1}{2}\gamma_T dt} \\ & + (dt^2/M_I)(\mathbf{F}_{BO}(t) + \mathbf{N}_I(t)(1 + \frac{1}{2}\gamma_T dt)^{-1}, \end{aligned} \quad (4)$$

The velocities of ions $\mathbf{v}_I(t + dt)$ can also be calculated by using the Verlet formula

$$\mathbf{v}_I(t + dt) = \dot{\mathbf{R}}_I = \frac{\mathbf{R}_I(t + dt) - \mathbf{R}_I(t - dt)}{2dt}. \quad (5)$$

This *ab initio* molecular dynamics model based on LE is named QLMD, which extends the applications of *ab initio* method into the field of HEDP. Based on QLMD, the effects of coupled ions and degenerate electrons can be studied, and give much more accurate results at relatively low temperature and high density. It is worth pointing out that the computational cost of the QLMD is very expensive under conditions of very weakly coupled and non-degenerate matter. In this case, the existing models such as MHD, ACTEX, and AA model can give consistent and accurate data.

2.2. Average atoms model with electronic energy-level broadening

The average atom model is one of the statistical approximations applied to study the electronic structure of atoms and ions in hot dense plasmas, which is easily to be applied in conjunction with a variety of treatments of electron orbitals in atoms. In a full relativistic self-consistent field-based AA model, the influence of the environment on the atom is assumed to be spherically symmetric on average. The movement of an electron under the interactions of the nucleus and other electrons is approximated by a central field, which is determined by the standard self-consistent calculation. In the central field, the radial part

of the Dirac equation has the form:

$$\begin{cases} \frac{dP_{n\kappa}(r)}{dr} + \frac{\kappa}{r}P_{n\kappa}(r) = \frac{1}{c}[\epsilon + c^2 - V(r)]Q_{n\kappa}(r) \\ \frac{dQ_{n\kappa}(r)}{dr} - \frac{\kappa}{r}Q_{n\kappa}(r) = -\frac{1}{c}[\epsilon - c^2 - V(r)]P_{n\kappa}(r) \end{cases} \quad (6)$$

where $P(r)$ and $Q(r)$ are respectively the large and small components of the wave function, c is the light speed, and $V(r)$ is the self-consistent potential, consisting of three parts, which are respectively the static, exchange and correlation potentials. The static part is calculated from the charge distributions in the atom, while the exchange and correlation parts take the approximate forms of Dharma-Wardana and Taylor ([Dharma-Wardana & Taylor 1981](#)).

For bound states, we have the boundary conditions satisfied by the radial wave functions

$$\begin{cases} P_{n\kappa}(r) \xrightarrow{r \rightarrow 0} ar^{l+1} \\ P_{n\kappa}(R_b) = 0 \end{cases} \quad \text{or} \quad \begin{cases} P_{n\kappa}(r) \xrightarrow{r \rightarrow 0} ar^{l+1} \\ \frac{d}{dr}\left[\frac{P_{n\kappa}(r)}{r}\right]_{R_b} = 0 \end{cases} \quad (7)$$

where R_b is the radius of the atom. The electron distribution is calculated separately for the bound and free electron parts. The bound electron density is obtained according to

$$D_b(r) = \frac{1}{4\pi r^2} \sum_j b_j (P_j^2(r) + Q_j^2(r)) \quad (8)$$

where b_j is the occupation number of the state j . In AA model without energy-level broadening, the occupation number b_j is determined by the Fermi-Dirac distribution

$$b_j = \frac{2|\kappa_j|}{\exp((\epsilon_j - \mu)/T) + 1}. \quad (9)$$

In order to consider the effect of energy-level broadening, Gaussian functions $\rho(\epsilon)$ centered at the corresponding electron orbital energies of Eq. 7 are introduced into the Fermi-Dirac distribution of electrons, i.e.,

$$b_j(\epsilon) = \frac{2|\kappa_j|\rho(\epsilon)}{\exp((\epsilon_j - \mu)/T) + 1} \quad (10)$$

and

$$D_b(r) = \frac{1}{4\pi r^2} \sum_j \int_a^b b_j(\epsilon) (P_j^2(r) + Q_j^2(r)) d\epsilon, \quad (11)$$

where $1 = \int_a^b \rho(\epsilon) d\epsilon$ and the two orbital energies obtained from the boundary conditions of Eq. 7 are taken as the upper and lower half maximum positions of the Gaussian form energy-level broadening.

Based on this approach, the splitting of the real energy levels approximated by the energy-level broadening can be considered, which makes the irregularities caused by the pressure-induced electron ionization without energy-level broadening disappear naturally (Hou et al. 2006, 2007).

3. Results and discussions

3.1. Computational details

For the study of solar interior EOS, we choose three typical densities in the solar interior: 10 g/cm³ (radiative zone), 100 g/cm³ and 160 g/cm³ (core). Temperatures from 1 eV to 550 eV for 10 g/cm³, and 10 eV to 1500 eV for 100 and 160 g/cm³ are calculated, covering the conditions from the radiative zone into the core. Since the H and He elements take up about 98% of the composition of the sun (Lodders 2003), we calculated four structures with different compositions (using X to represent the mass abundance of H, and Y for abundance of He, Z for others), which are X=1, Y=0, Z=0; X=0, Y=1, Z=0; X=0.7, Y=0.3, Z=0; X=0.40, Y=0.60, Z=0. The supercells containing T=125 particles for 10 g/cm³ and T=256 particles for 160 g/cm³ are constructed. When Z=0, the number of H atoms (N_H) and He (N_{He}) can be calculated by the formulas:

$$\frac{4N_{He}}{4N_{He} + N_H} = Y, N_{He} + N_H = T \quad (12)$$

In these conditions, the matter goes from strongly coupled to relatively weakly coupled, and from partially degenerate to weakly degenerate, as shown in Fig. 1, where QLMD has been proved successfully.

For the QLMD simulations, we have used the Quantum Espresso package (Giannozzi et al. 2009) based on the finite temperature DFT. The Perdew-Zunger parametrization of local density approximation (LDA) (Perdew & Zunger 1981) is used for the exchange-correlation potential. Similar to the calculation of Hydrogen at the density of 80 g/cm³ (Dai et al. 2010; Recoules et al. 2009), the Coulombic pseudopotentials with a cutoff radius of 0.005 a.u. for H and He are adopted. The plane wave cutoff energy is set to be from 200 Ry to 400 Ry with the increase of temperature. As discussed in Ref. (Recoules et al. 2009), pressure delocalization promises that the upper band electronic eigenstates are nearly plane waves, and thus the basis set is greatly reduced. Therefore, even though we choose a large number of bands in order to ensure the accuracy of the calculation, the computational cost is not very expensive. In our cases, we used enough bands in order to make the corresponding band energies higher than $8k_B T$ (especially at high temperature). Gamma point only is used for the representation of the Brillouin zone. We tested all these parameters carefully, and found that more k-points, more bands, larger energy cutoff, and more particles do not give any significant difference. The time step of QLMD is $a_I/(20\sqrt{k_B T M_I})$ (Recoules et al. 2009), where a_I and M_I are the average ionic radius and the ionic mass of I_{th} ion, respectively. After thermalization, each structure is simulated for 5000 to 10000 time steps to pick up the useful information.

3.2. Equation of state

Firstly, we study the isochoric heating curve along the density of 10 g/cm³ from 1 eV to 550 eV under the conditions of the solar radiative zone. Comparisons between the pressure calculated using QLMD and AAB models for different compositions are given in Fig. 2. It is shown that for the system of He with two electrons at lower temperatures, the pressure of AAB model is much larger than that of QLMD. However, the relative difference

for H is not as big as for He. Therefore, with the increase of temperature and abundance of Hydrogen, the gap between QLMD and AAB models becomes less and less. It is very clear that more electrons and low temperature result in difficulties of describing the ionization balance for AAB model, where the composition of the system is complicated. The strong coupling among the ions, which is included in QLMD model but not in AAB model, plays an important role too in the calculations. Here, we recall that the simple way to calculate the EOS containing only one element and averaging the pressure according to the mass ratio is not accurate enough, as discussed in Ref. (Yuan 2002). For example, for the density-temperature point (10 g/cm³, 10 eV) and composition (X=0.7, Y=0.3, Z=0), the average pressure is $P_a = (0.7 \times 301.3 + 0.3 \times 58.6) = 228.49$ Mbar. However, the pressure of this mixture obtained using QLMD is 214.77 Mbar, and the error is about 6%, which is significant for astrophysical applications.

When the conditions go further into the solar interior, some interesting characteristics appear. For the density of 100 g/cm³, pressure-temperature relation is shown in Fig. 3. Moreover, the maximum density of the sun is about 160 g/cm³, whose isochoric heating curve from 10 eV to 1500 eV is shown in Fig. 4. Contrary to the relative difference between QLMD and AAB models in Fig. 2, the pressures of AAB model for 100 and 160 g/cm³ are smaller than those of QLMD model, especially for one component H. In fact, the spherical assumption (Yuan 2002) for ions in AAB model makes the effective volume of the system larger than the real one, giving rise to smaller pressure. This phenomenon is obvious when the density is high enough, such as 160 g/cm³ for H here. With the increase of temperature, the pressure of AAB and QLMD becomes consistent. At high temperatures, the ions are weakly coupled and electrons are almost free. Therefore, the semiclassical methods such as Thomas-Fermi and AAB can work well. Furthermore, it can be deduced that the EOS of the whole area of the sun can be obtained accurately and smoothly, which is beyond the OP and OPAL models, and completely parameter-free.

For the central conditions in the sun, the density reaches up to 152.7 g/cm^3 and the temperature up to 15696000 K according to the standard solar model (Bahcall et al. 2001). The central pressure is also about $2.342 \times 10^5 \text{ Mbar}$, which is never reached from first principles simulation before. Based on QLMD, we solved this problem from an *ab initio* approach and obtained the EOS under this condition. We firstly compared the pressure close to the solar center with other models, as shown in Table. 1, and they agree reasonably well with each other. It is interesting to find that the pressure of AA model without energy-level broadening (AANB) is much larger than those of QLMD and AAB, and consistent with other models of EFF, Livermore (LIV) and MHD (Däppen et al. 1990). Since QLMD can be realized much more reliably, we can think AAB more reasonable, and both QLMD and AAB can improve the accuracy of EOS much. In fact, for the very dense medium, the electronic structures of elements are not only the energy levels, but also energy bands. It is reasonable to consider the effect of energy-level broadening, which is naturally included in QLMD and thus gives rise to appropriate results. For the solar central regime, we calculate the pressure with different compositions. First of all, we consider the chemical compositions of H and He, with abundances $X=0.34828$, $Y=0.65172$, $Z=0.0$. It is found that the pressures of QLMD and AAB are almost equal within 0.5% error and are very similar to that of Standard. The small difference is caused by the lack of the heavier elements. In order to understand the effect of heavier elements on the EOS, we study the pressure of chemical compositions of H, He, C and H, He, O, respectively. As shown in Table. 1, the existence of heavier elements decreases the pressure a little, since the abundance is very small. In principle, we can calculate the conditions of solar interior with any composition and any abundance using QLMD resulting in EOS accurately and smoothly, particularly at relatively low temperatures and high densities. QLMD can also be very complementary to the AA models considering the computational cost, and improve significantly the accuracy of EOS in the solar interior.

In conclusion, the EOS of solar interior is calculated based on first principles method named QLMD, which is beyond the MHD and OPAL models. Furthermore, the model of QLMD can promise the accuracy for the EOS and be complementary to AA-like models. The accuracy can be improved significantly, particularly at relatively low temperatures and high densities where the coupling of ions can not be neglected. This gives us a useful tool to investigate the properties of the sun and sun-like stars from *ab initio* approaches, which is very powerful in astrophysics. This work can also open a new field to investigate the solar or stellar properties from first principles, promoting the study in astrophysics both in theory and experiment.

This work is supported by the National Natural Science Foundation of China under Grant Nos. 10734140, 60921062 and 10676039, the National Basic Research Program of China (973 Program) under Grant No. 2007CB815105. Calculations are carried out at the Research Center of Supercomputing Application, NUDT. The authors thank the comments of the anonymous reviewer.

REFERENCES

- Basu, S., & Antia, H. M. 2008, Phys. Rep. 457, 217
- Berrington, K. A. 1997 *The Opacity Project, vol. II*. (Bristol: Institute of Physics)
- Collins, L. *et al.*, 1995, Phys. Rev. E, 52, 6202
- Dai, J., & Yuan, J. 2009, Europhys. Lett. 88, 20001
- Dai, J., Hou, Y., & Yuan, J. 2010, Phys. Rev. Lett., 104, 245001
- Däppen, W., Mihalas, D., Hummer, D. G., & Mihalas B. W. 1988, ApJ, 332, 261
- Däppen, W., Lebreton, Y., & Rogers, F. 1990, Solar Physics, 128, 35
- Däppen, W., & Nayfonov, A. 2000, Astrophys. J. Suppl. Ser. 127, 287
- Däppen, W. 2006 J. Phys. A: Math. Gen. 39, 4441
- Desjarlais, M. P. *et al.*, 2002, Phys. Rev. E, 66, 025401(R)
- Dharma-Wardana, M. W. C., & Taylor, R., J. Phys. C: Solid State Phys. 14, 629
- Eggleton, P., Faulkner, J., & Flannery, B. P. 1973, Astron. Astrophys. 23, 325
- Faussurier, G., Blancard, C., Cossé, P., & Renaudin, P. 2010, Phys. Plasmas, 17, 052707
- Giannozzi, P. *et al.*, 2009, J. Phys.: Condens. Matter, 21, 395502; www.quantum-espresso.org
- Gillan, M. J., Alfè, D., Brodholt, J., Vocadlo, L., & Price, G. D. 2006, Rep. Prog. Phys. 69, 2365
- Hou, Y., Jin, F., & Yuan, J. 2006, Phys. Plasmas 13, 093301

- Hou, Y., Jin, F., & Yuan, J. 2007, J. Phys.: Condens. Matter, 19, 425204
- Hummer, D. G., & Mihalas, D. 1988, ApJ, 331, 794
- Ichimaru, S. 1982, Rev. Mod. Phys., 54, 1017.
- Iglesias, C. A., & Rogers, F. J. 1991, 371, 408
- Iglesias, C. A., & Rogers, F. J. 1993, ApJ, 412, 752
- Iglesias, C. A., & Rogers, F. J. 1995, ApJ, 443, 460
- Iglesias, C. A., & Rogers, F. J. 1996, ApJ, 464, 943
- Lodders, K. 2003, ApJ, 591, 1220
- Lorenzen, W., Holst, B. & Redmer, R. 2009, Phys. Rev. Lett., 102, 115701
- Mazevet, S. *et al.*, 2005, Phys. Rev. E, 71, 016409
- Mazevet, S. *et al.*, 2008, Phys. Rev. Lett., 101, 155001
- Mihalas, D., Däppen, W., & Hummer, D. G. 1988, ApJ, 331, 815
- Militzer, B. & Hubbard, W. B. 2009, Astrophys Space Sci. 322, 129
- Bahcall, J. N., Pinsonneault, M. H., & Basu, S. 2001, ApJ, 555, 990
- Nayfonov, A., Däppen, W., Hummer, D. G., & Mihalas, D. M. 1999 ApJ, 526, 451
- Nettelmann, N., Holst, B., Nettelmann, A., French, M., & Redmer, R. 2008, ApJ, 683, 1217
- Perdew, J. P. & Zunger, A. 1981, Phys. Rev. B, 23, 5048
- Pastor, R. W., Brooks, B. R. & Szabo, A., 1988, Mol. Phys., 65, 1409

- Recoules, V., Lambert, F., Decoster, A., Canaud, B., & Cl  rouin, J. 2009, Phys. Rev. Lett., 102, 075002
- Rogers, F. J. 1986, ApJ, 310, 723
- Rogers, F. J., Swenson, F. J., & Iglesias C. A. 1996, ApJ, 456, 902
- Rogers, F. J., & Nayfonov, A. 2002, ApJ, 576, 1064
- Seaton, M. J. 1995, *The Opacity Project, vol. I.* (Bristol: Institute of Physics)
- Trampedach, R., D  ppen, W., & Baturin, V. A. 2006, ApJ, 646, 560
- Vorberger, J., Tamblyn, I., Militzer, B., & Bonev, S. A. 2007, Phys. Rev. B, 75, 024206
- Wilson, H. F., & Militzer, B. 2010, Phys. Rev. Lett. 104, 121101
- Yuan, J. 2002, Phys. Rev. E, 66, 047401
- Zeng, J., & Yuan, J. 2004, Phys. Rev. E, 70, 027401

Table 1: Comparison of central pressures of the sun at typical temperature (T) and density (ρ). The results of EFF, LIV (OPAL) and MHD are in Ref. (Däppen et al. 1990) (X=0.34828, Y=0.65172, Z=0). Results of AANB, AAB, and standard solar model (Standard) (Bahcall et al. 2001) are also compared. The pressures of chemical composition of H, He and C with X=0.3387, Y=6613, Z=0 (^a), X=0.3125, Y=0.6406, Z=0.0469 (^b), and chemical composition of H, He and O with X=0.3077, Y=0.6308, Z=0.0615 (^c) are also shown.

ρ (g/cm ³)	T (eV)	EOS model	pressure (Mbar)
141.25	989.45	EFF	1.6396×10^5
		LIV	1.6162×10^5
		MHD	1.6190×10^5
		AANB	1.6144×10^5
		AAB	1.5922×10^5
		QLMD	1.6090×10^5
141.25	1189.58	EFF	1.9579×10^5
		LIV	1.9337×10^5
		MHD	1.9365×10^5
		AANB	1.9330×10^5
		AAB	1.9027×10^5
		QLMD	1.9122×10^5
152.70	1352.64	Standard	2.3420×10^5
		AANB ^a	2.3603×10^5
		AAB ^a	2.3417×10^5
		QLMD ^a	2.3525×10^5
		AANB ^b	2.2678×10^5
		AAB ^b	2.2534×10^5
		QLMD ^b	2.2575×10^5
		AANB ^c	2.2445×10^5
		AAB ^c	2.2301×10^5
		QLMD ^c	2.2328×10^5

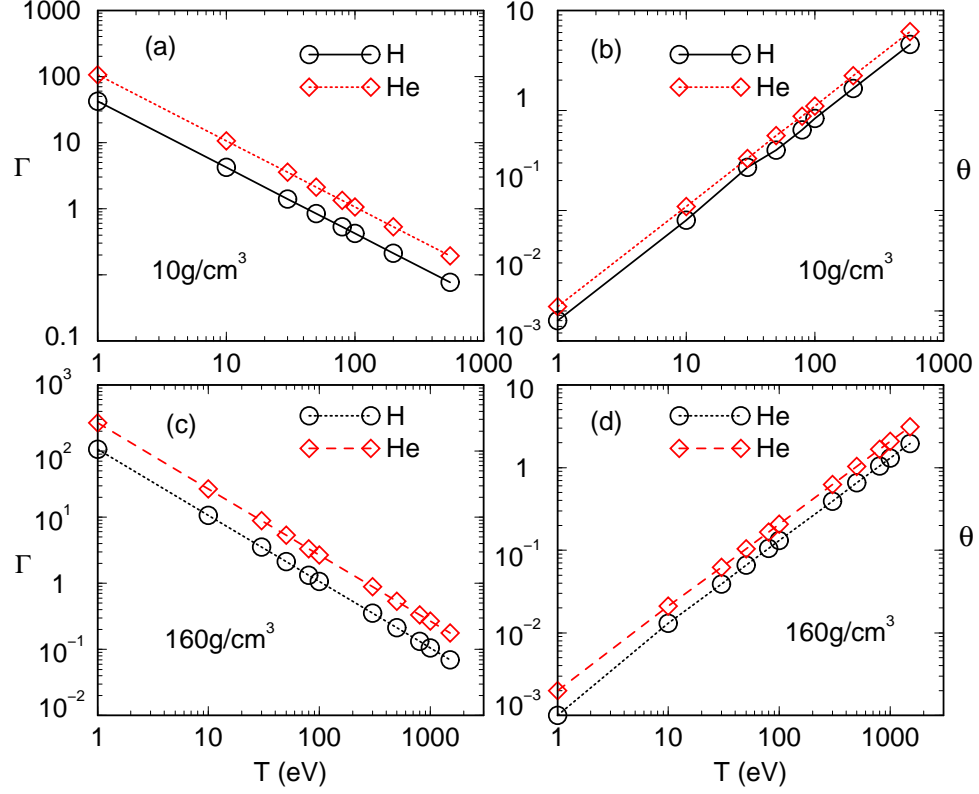


Fig. 1.— (Color online) The coupling parameters (Γ) and degenerate parameters (θ) of H and He from 1 eV to 550 eV at 10 g/cm^3 (a)-(b), and from 10 eV to 1500 eV at the density of 160 g/cm^3 (c)-(d).

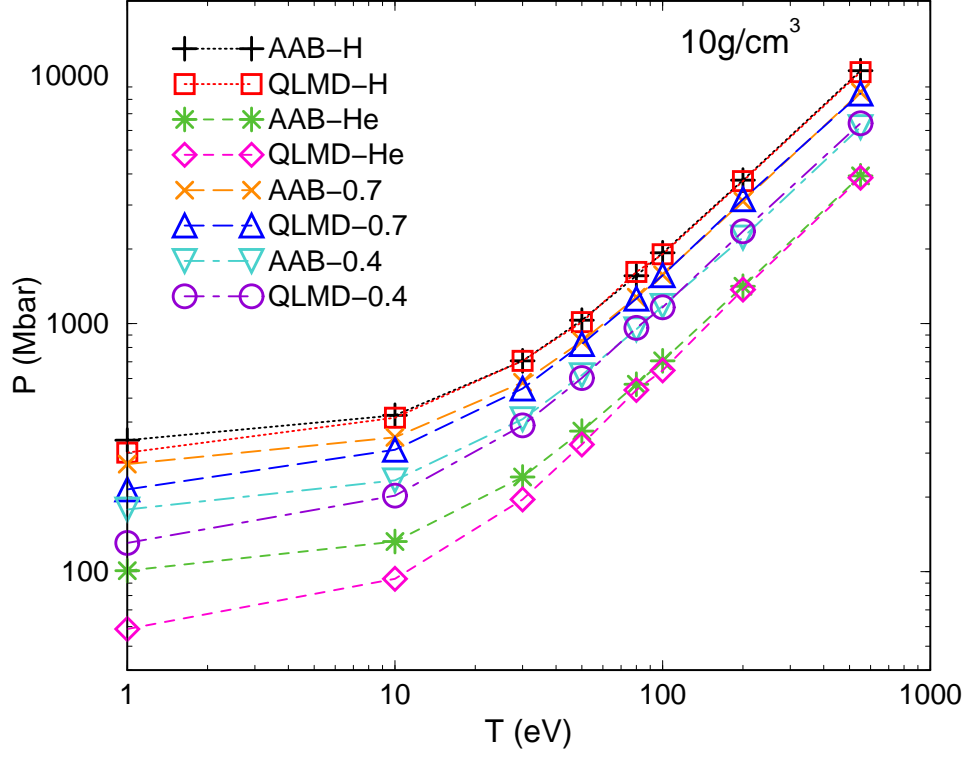


Fig. 2.— (Color online) Pressure vs temperature for the density of 10 g/cm³ with different chemical compositions compared with results of AAB. In the figure, 0.7 represents X=0.7, 0.4 represents X=0.4, respectively.

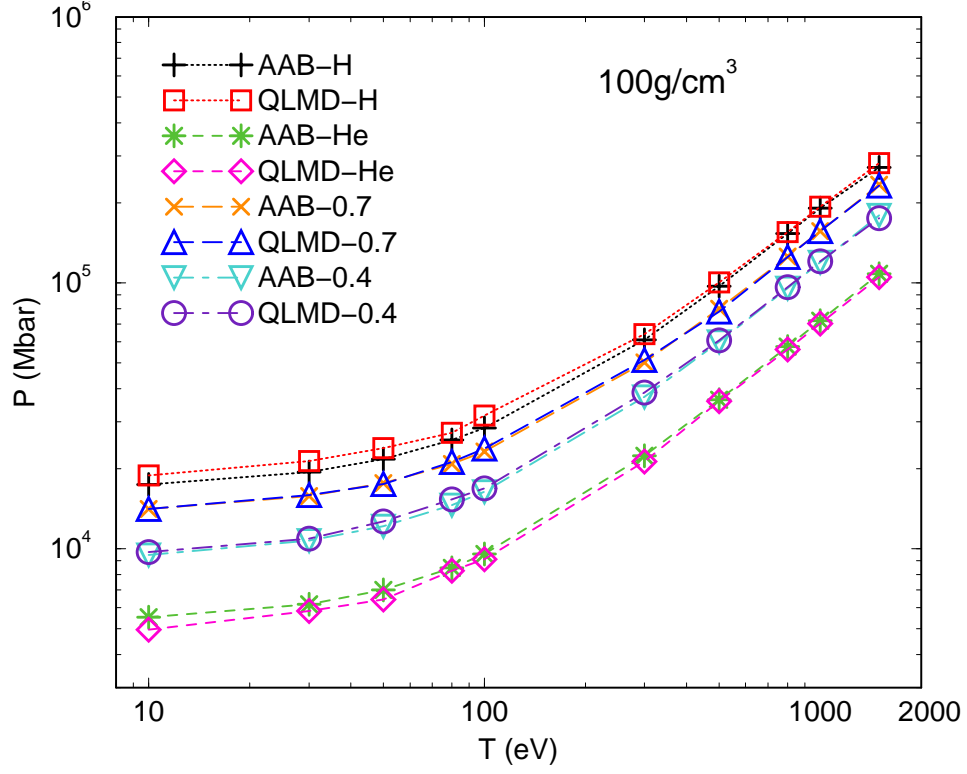


Fig. 3.— (Color online) Pressure vs temperature for the density of 100 g/cm³ with different chemical compositions compared with results of AAB.

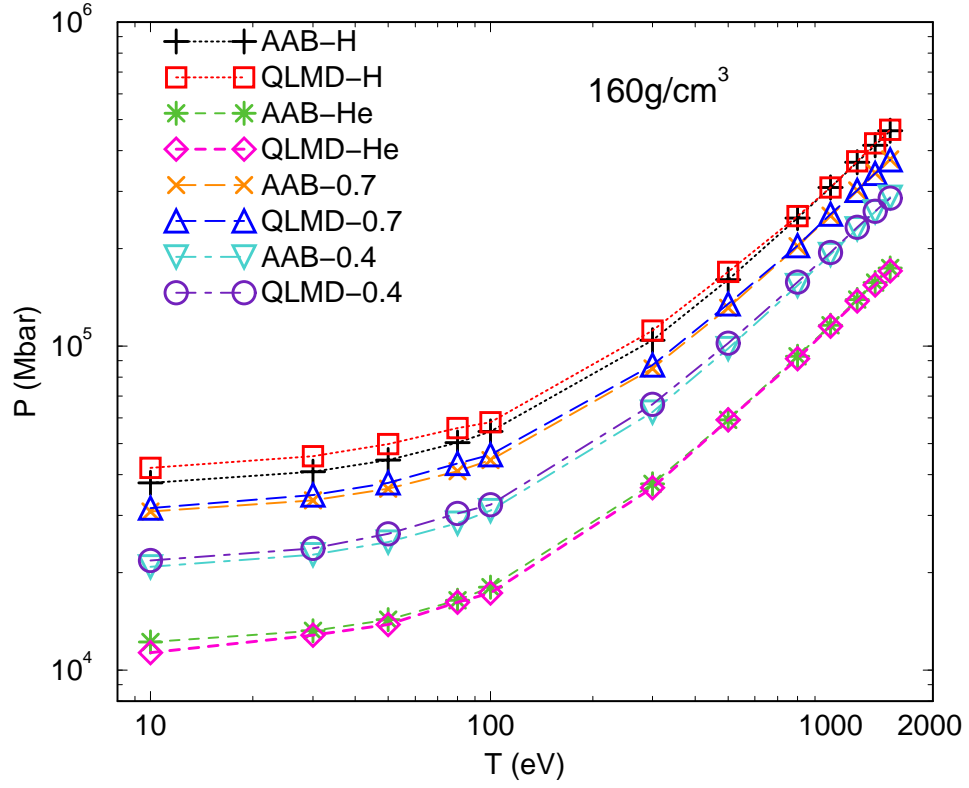


Fig. 4.— (Color online) Pressure vs temperature for the density of 160 g/cm³ with different chemical compositions compared with results of AAB.